

CHAPTER 2

Theory

2.1 Binary star systems

2.1.1 Classification of binary stars

Binary stars are systems of two stars orbiting around each other in their common center of mass. The brighter star is called primary star and the other is called secondary star. About half of observable stars are binary systems. They can be divided from their characteristics to 4 types.

- 1) **Visual binaries** A visual binary is a binary system which the component stars are widely separated by tens to few hundred AU and orbital periods range from hundreds of days to as long as centuries. The stars in such systems are gravitationally bound to each other and do not interact. The changing of relative position of the stars can be observed by telescope.
- 2) **Eclipsing binaries** The binary systems that cannot be separated by each component of the system but can notice from the “Light curve” are called Eclipsing binaries. This change of the brightness is because of the relative orbital motion of the components. The analysis of a curve provide the inclination of a system, the ratio of luminosities, the photometric mass ratio and the information of their shapes. The absolute parameters can be determined from its photometric and spectroscopic observations.
- 3) **Astrometric binaries** The binary stars which one star is much brighter than the other component and both stars are too close each other. It is called Astrometric binaries. So, only one star can be observed directly but the other

component can be found out from the oscillatory motion of the brighter component.

- 4) **Spectroscopic binaries** component of this type of binary systems cannot be observed separately. But the motion can be notice from a line shift in the spectrum which occur from “Doppler Effect”. There are two subgroups of spectroscopic binaries, the single-lined spectroscopic binary (SB1), where only one component can be detected from the spectrum, and the double-lined spectroscopic binary (SB2) where both spectra are observed. In some binary systems, the component itself also vary in its brightness from its intrinsic variation. Those types of variable component are including RS CVn-type.
- 5) **RS CVn stars** The RS CVn type binaries represent a class of close detach active binaries that rotate synchronously due to tidal forces. These system is consist with the massive primary component (mostly G-K) and the secondary subgiant or dwarf (G-M). They show optical variability which is characterized by a large amplitude and interpreted as rotational modulated effect of cool spots on their surfaces. Because of low luminosity of the secondary component, where both component can be observed, the primary component is brighter than the secondary and appear as single-line binaries.

Table 2.1: The catalog of RS CVn systems characteristic.

Type of system; mass ratio ($q = m_2/m_1$)	Spectral range orbital period	Photometric features	Spectral features
RS CVn systems (e.g., RS CVn)	Primary: GV Secondary: KIV	Two well-defined eclipses, but distortions due to extensive starspots	SB2 with optical/UV emission; soft x-ray and radio emission; chromospheric mass loss
Detached $q \approx$ 0.7-1.2			

2.1.2 Geometry of binary systems

We shall first consider a Doppler Effect equation that was originally studied in the visible part of the spectrum. In astronomy, the Doppler shift, as Doppler Effect, applies

to electromagnetic waves in all portions of the spectrum. Also, because of the inverse relationship between frequency and wavelength, we can describe the Doppler shift in terms of wavelength as show in this equation,

$$\frac{\lambda - \lambda_0}{\lambda} = \frac{\Delta\lambda}{\lambda} = \left[\frac{1 + (V_{rad}/c)}{1 - (V_{rad}/c)} \right]^{1/2} - 1 \approx \frac{V_{rad}}{c} \quad (2.1)$$

Where V_{rad} is the radial velocity relative to the observer, which is much less than c , the speed of light, λ is the observed wavelength of a line and λ_0 is the rest wavelength. For a receding star, the radial velocity is positive when the spectrum is redshift. The radial velocity is negative when the star is approaching and the spectrum is blueshifted.

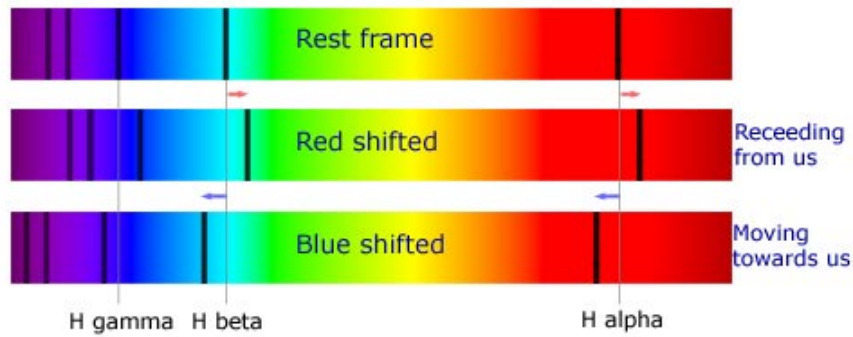


Figure 2.1: The example spectra are showing relation between the shifted line and object motion which refer with the rest frame. (Diagram from http://www.atnf.csiro.au/outreach/education/senior/astrophysics/spectra_info.html)

In figure (2) was presented the orientation of the binary orbit in space relative to the line of sight of the observer, Oz , and the tangent plane of the sky. The polar coordinates of the star at P_2 with respect to O are $(r, \theta + \omega)$, which can be resolved into two component in the orbital plane: $r \cos(\theta + \omega)$ along the line of nodes NON' , and $r \sin(\theta + \omega)$ at a right angle to NON' . When the second quantity were projected into the line of sight Oz , it could be obtained

$$z = r \sin(\theta + \omega) \sin i \quad (2.2)$$

Hence, the observed radial velocity due to orbital motion is

$$V_{rad} = \dot{z} = \sin i [\sin(v + \omega)\dot{r} + r \cos(v + \omega)\dot{v}] + \gamma$$

$$\begin{aligned}
&= \frac{2\pi a \sin i}{P(1 - e^2)^{1/2}} [\cos(v + \omega) + e \cos(\omega)] + \gamma \\
&= K[\cos(\theta + \omega) + e \cos(\omega)] + \gamma
\end{aligned} \tag{2.3}$$

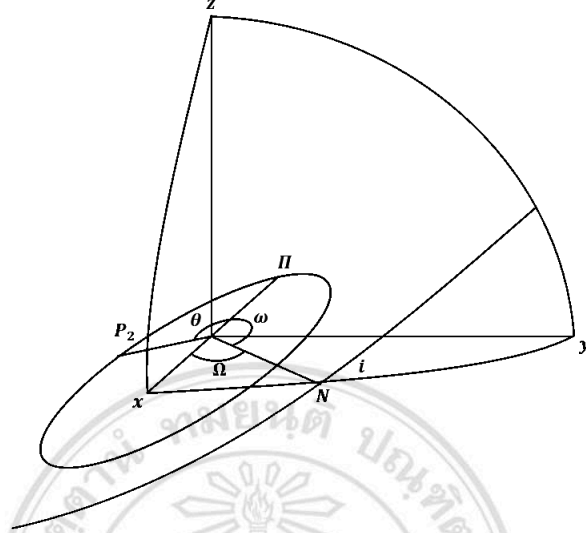


Figure 2.2: The relative orbit of a binary located in three dimensions and defined by the angle Ω , ω and i . (Hildith, 2001)

where a is the semi-major axis, i is the inclination of the system, e is the orbital eccentricity, θ is the true anomaly and ω is the longitude of periastron. The parameter $K = [2\pi a \sin i]/[P(1 - e^2)^{1/2}]$ is called the semi-amplitude of the radial velocity curve, and γ is the systemic velocity or the radial velocity of the centre of mass of the binary system.

For constant values of the quantities γ , K , e , and ω , the radial velocity V_{rad} of one component of a binary is a maximum, when $(v + \omega = 0)$ or at minimum, when $(v + \omega = \pi)$. That is, when the star is at the ascending node N or at the descending node N' when $(v + \omega = 0)$ or $(v + \omega = \pi)$, respectively. If the star has $e = 0$, equation (2.2) gives a cosine curve, as shown in figure 2.3.

As e increase, the velocity curve becomes increasingly skew-symmetric, as illustrated in figure 2.4.

Spectroscopic binary data can be used to determined mass ratio of the system even the inclination of the system is unknown. The semi-major a is the sum of the semi-major

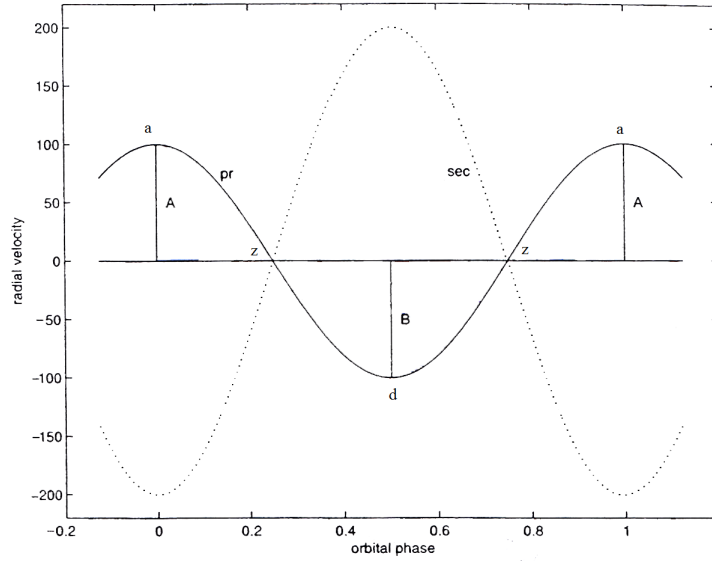


Figure 2.3: The example of radial-velocity curves for the two stars in a binary system with a circular orbit. The semi-amplitudes are $K_1 = 100$ km/s and $K_2 = 200$ km/s, giving a mass ratio $q = m_2/m_1 = 0.5$. The systemic velocity is $\gamma = 0$ km/s. The positions of the ascending (a) and descending (d) nodes are shown and the points of zero (z) orbital radial velocity. In the upper panel, the observer views the binary orbit from the right along z-z.

axis of each component:

$$a = a_1 + a_2 \quad (2.4)$$

If e is much less than 1 (nearly circular orbit), the velocity of system can be estimated as:

$$v_1 = 2\pi a_1/P, v_2 = 2\pi a_2/P$$

Hence, Equation (2.4) become

$$a = \frac{P}{2\pi}(v_1 + v_2) \quad (2.5)$$

Form the Kepler's third law

$$m_1 + m_2 = \frac{P}{2\pi G}(v_1 + v_2)^2, \quad (2.6)$$

if consider the radial velocity $v_1 \sin i = v_{1r}, v_2 \sin i = v_{2r}$, then

$$m_1 + m_2 = \frac{P}{2\pi G} \frac{(v_{1r} + v_{2r})^3}{\sin^3 i}. \quad (2.7)$$

There are many spectroscopic binary with one component much brighter than another component. It can be observed only one set of spectral lines. They are called Single-line

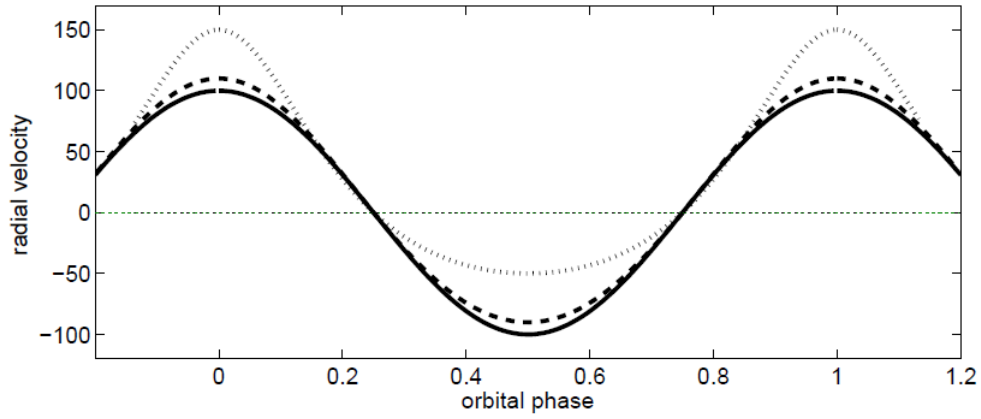


Figure 2.4: The radial velocity of a circular orbit ($e = 0$, solid line), and elliptical orbits. The dashed line represent the curve of $e = 0.1$ and $\omega = 0^\circ$ and the dotted line represents the curve of $e = 0.5$ and $\omega = 0^\circ$. The semi-amplitude of all curves is $K = 100$ km/s and $\gamma = 0$ km/s. (Komonjinda, 2008)

spectroscopic Binary.

If the inclination is know from another kind of observation, the mass ratio and the semi-major axis of a system can be determined. For this case, the equation is limited radial velocity of the secondary component (v_{2r})

$$m_1 + m_2 = \frac{P}{2\pi G} \frac{(v_{1r})^3}{\sin^3 i} \left(1 + \frac{m_1}{m_2}\right)^2 \quad (2.8)$$

where $\frac{m_1}{m_2} = \frac{v_{2r}/\sin i}{v_{1r}/\sin i} = \frac{v_{2r}}{v_{1r}}$,

thus,

$$\frac{m_2^3}{(m_1 + m_2)^2} \sin^3 i = \frac{P}{2\pi G} v_{1r}^3. \quad (2.9)$$

In the left hand side of equation (2.8) is called **Mass Function** of single-line spectroscopic binary which depends on only two value, period (P) and radial velocity of one component (v_{1r}).

2.2 Spectroscopy

Spectroscopy is one of the fundamental tools at an astronomer's disposal. It allows one to determine many information about astronomical objects, such as chemical composition, physical properties and radial velocities. The light is composed of many wavelength in different colores and cannot resolved into spectrum by eyes. Spectroscopy is based on measurement of absorption lines. All of these measurements of spectrum lines includes the Doppler effect. It make possible for astronomers to determine the physical conditions of distant stars.

2.2.1 Black body radiation

The black body theory of thermal emission was proposed to demonstrate the thermal properties of a body in equilibrium. The distribution of light emitted by a body will follow a regular shape depends on its temperature. This is the black body curve

When the body is heated, the peak wavelength of the light emitted varies, peaking initially in the infrared and moving towards the UV. A dull is normally visible when material is heated to around 800°C, as the temperature increase, the colores becomes orange and eventually white (white hot). Wein and Planck later developed the mathematical model for this transition, which can be simply stated as

$$\lambda_{max} = 2.897 \times 10^6 \frac{1}{T} \quad (2.10)$$

where T is the tempereture in degree *Kelvin*, and λ_{max} the peak emission wavelength in nanometer unit, see figure 2.5

The shape of the spectrum reflects the surface temperature of the star. It is assumed that star or any material act like black bodies. The Planck curve shows that the position of the peak energy moves toward the blue region with increasing temperature and also moves toward the red region when the temperature is decreased.

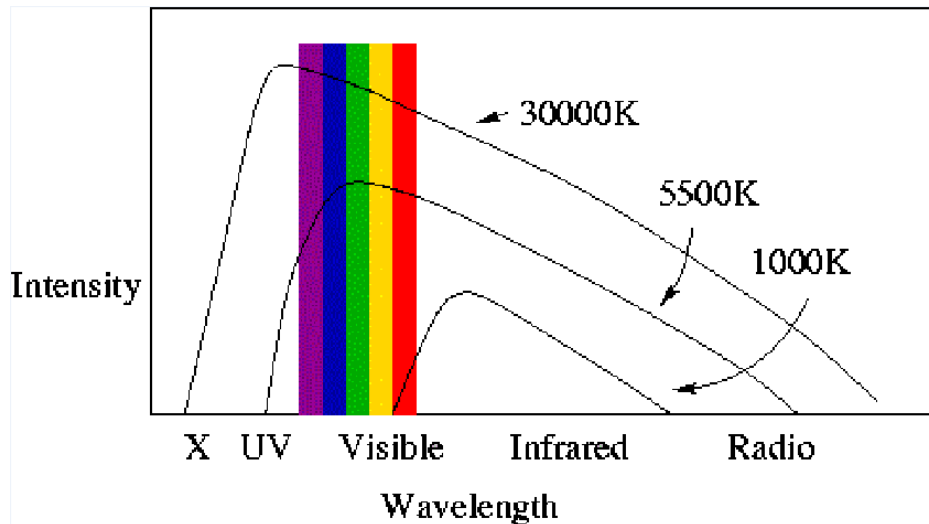


Figure 2.5: Showing the dispertional energy compare with wavelength at difference temperatures scale according to Planck's law. (Diagram from <http://www.ucolick.org>)

2.2.2 Spectral profile (The stellar rotational velocity)

Stellar rotation has an effect on the absorption line of a star which cause the light coming from the different parts of the stellar disc. The line can be broadened depending on the rotation of star which relative with the rotational velocity and the orientation of the rotational axis figure 2.6. A star with a more inclination of rotation axis to the line-of-sight, the absorption line will more broaden. On the other hand, the line will have a zero effect if a star axis is parallel to the line-of-sight.

Rotational velocity, $v \sin i$, is defined as projected rotational velocity of the star. A star with higher $v \sin i$ will have a greater difference between blue and red shifted because of approaching limb and receding limb.

To measure the projected rotational velocity, $v \sin i$, it is necessary to compare the stellar line profile with a computed model. As described in *Gray (1992)*[7], by assuming a limb-darkening law of the function

$$I_c/I_0 = 1 - \epsilon + \epsilon \cos \theta \quad (2.11)$$

where I_c and I_0 are the intensity at a point on the surface and at the centre of the disk, respectively, and θ is the angle between the local normal and the line-of-sight. So, the

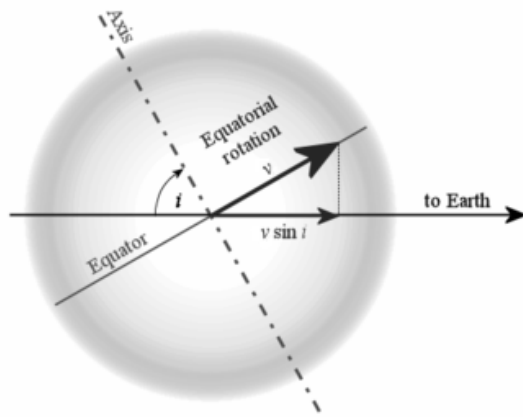


Figure 2.6: The star has inclination i to the line-of-sight of an observer on the Earth and rotational velocity v at the equator. (Diagram from <http://en.wikipedia.org/wiki/Stellarrotation>)

rotational broadening function can be written as

$$G(\Delta\lambda) = \frac{2(1 - \epsilon)[1 - (\Delta\lambda/\Delta\lambda_L)^2]^{1/2} + \frac{1}{2}\pi\epsilon[1 - (\Delta\lambda/\Delta\lambda_L)^2]}{\pi\Delta\lambda_L(1 - \epsilon/3)} \quad (2.12)$$

where λ is the rest wavelength of the absorption line,

$\Delta\lambda$ is the Doppler shift in this wavelength,

$\Delta\lambda_L$ is the maximum Doppler shift at the limb,

ϵ is the limb darkening coefficient.

The effect of stellar rotation on the line broadening profile is illustrated in figure 2.7. In this figure, theoretical line profiles as a function of $v \sin i$ at a wavelength 6122.23 Angstrom and $\epsilon = 0.6$ are shown. The line becomes broad and shallow with the larger rotational velocity.

According to broadening line profile, if the star is a fast rotation, the spectral line with neighbour can be blended with each other and the intensity become higher.

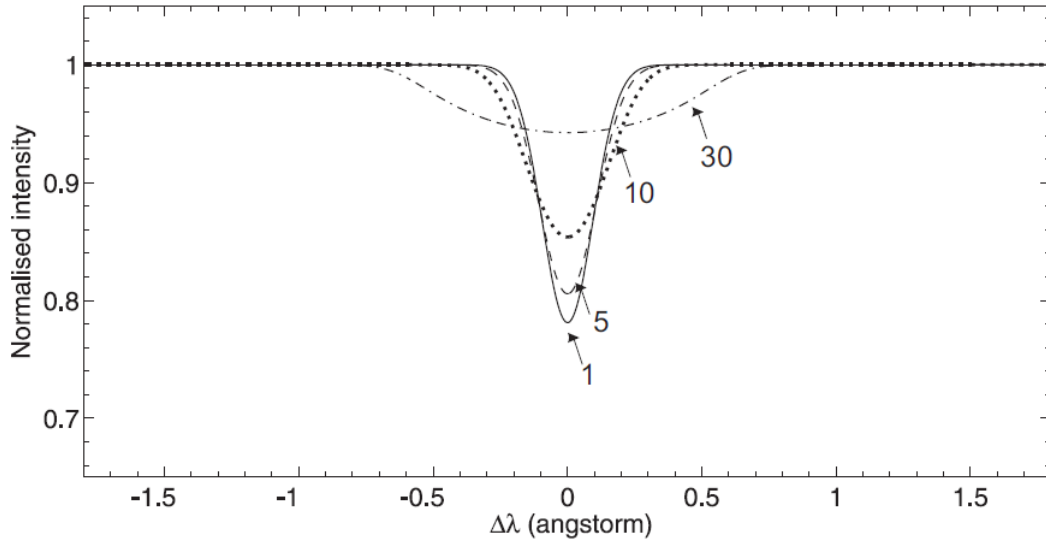


Figure 2.7: The computed line profiles as broadened from the rotation of a star. The labels are the value of $v \sin i$ in km/s. (Komonjinda, 2008)

2.2.3 Standard spectral lines and telluric lines

To accurately calibrate the spectrum, a series of reference lines can be used to measure the dispersion of the spectroscope and its resolution. The Balmer series of hydrogen are used to calibrate lines in the spectrum itself. The formula for the series is

$$1/\lambda = 109677.1(1/n^2 - 1/m^2) \quad (2.13)$$

where $n = 2$ for the Balmer series and m is an integer $> n$.

Table 2.2: The Balmer series of hydrogen.

m	Wavelength (Å)
$3H\alpha$	6563
$3H\beta$	4861
$3H\gamma$	4340
$3H\delta$	4102
$3H\epsilon$	3970
$3H\zeta$	3889
<i>9etc</i>	3855
<i>10etc</i>	3799

Moreover, there are also strong lines to use as reference lines such as Sodium doublet 5890 and 5896 Angstrom and telluric lines

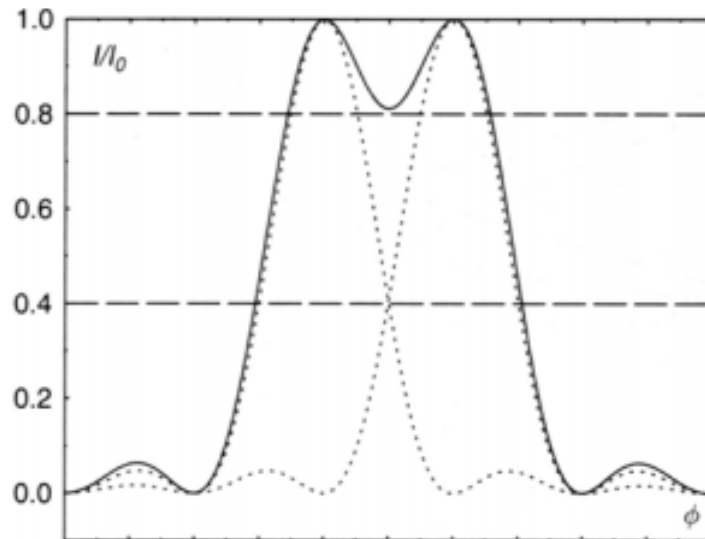


Figure 2.8: The blended line that occur from broadening line with the other. (Komonjinda, 2008)

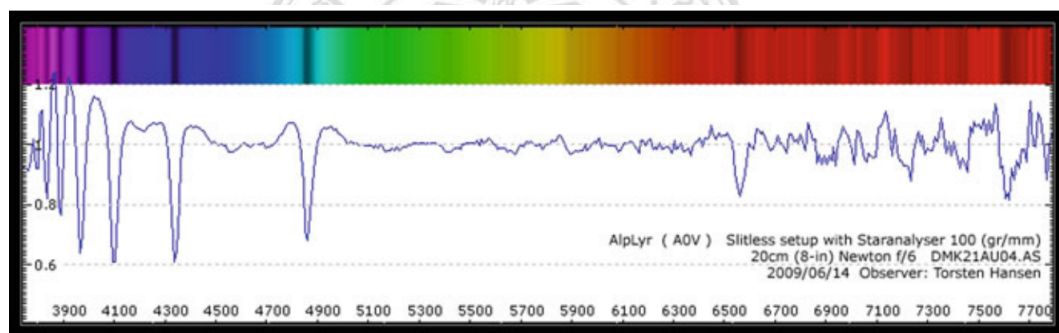


Figure 2.9: The example spectrum of Vega (Henson) is showed the reference lines according to Balmer series. (Diagram from Astronomical Spectroscopy for amateurs)

Telluric contamination occurs to astronomical spectra due to Earth's Atmospheric. Telluric absorption is simply the absorption of electromagnetic wavelengths by atmosphere molecules. The primary causes of telluric absorption are O_2 which absorb strongly in the near-UV region and H_2O which absorbs strongly and weak at many wavelength, especially in the yellow and red regions.

The strongest lines occur in the A-band (7600-7630 Å), in the B-band (6800-6890 Å), and also between 7170 and 7350 Angstroms.

Normally, these telluric lines will be avoided from the observer to obtain information from the object. On the other hand, as we also know, although the telluric lines are

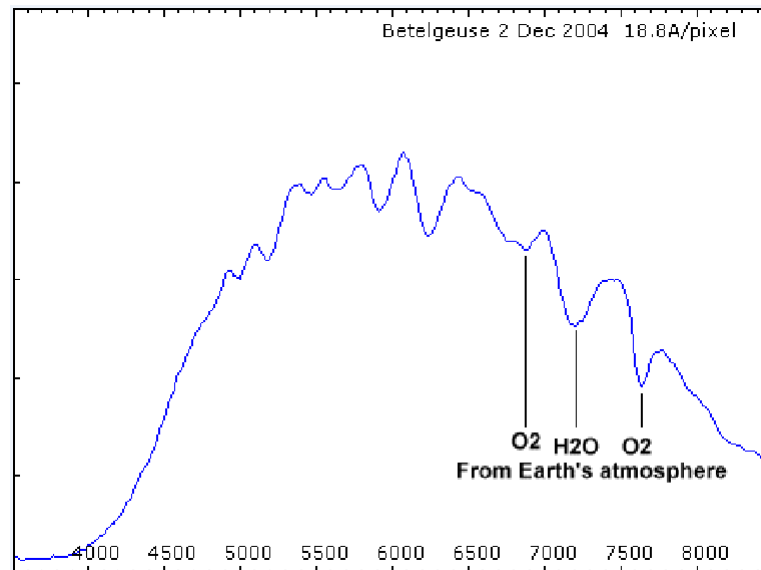


Figure 2.10: Telluric absorption lines due to oxygen water in the Earth's atmosphere. (Diagram from http://www.threehillsobservatory.co.uk/astro/spectra_9.htm)

occurred from Earth's orbital but still to be assumed at the rest wavelengths. So these telluric lines can be referenced to check the deviation of the observed spectrum.

2.2.4 Barycentric velocity and heliocentric correction

All of astronomical observations are made from continuously moving platforms, our Earth need to know what the motions are, and the Earth-based observations must be correct for the effect of those motions. The Sun can be adopted as a reference point, and because the observations obtained from the Earth orbit, *Barycentric velocity* and *heliocentric correction*, that involve measurement of time and velocity, are required to calculate for each particular observation.

This correction term is imply the projection of the Earth's orbital motion into the line of sight to the astronomical source at the time of the observation. The range of values of this correction for the Earth's orbital motion reaches a maximum range for sources that lie on the ecliptic, namely, ± 30 km/s. The Earth's rotation is located in elliptical coordinate, the range of value ± 0.46 km/s depending on the location of observatory.

2.3 Instrument: Spectrograph

2.3.1 Introduction to spectrographs

The spectrograph is an instrument that used to separate an incoming light from any object into its component wavelengths. Incoming light can be disperse or split into a spectrum, using a prism or diffraction grating.

Most spectrograph have a slit. Only one point source in the telescope's field of view can enter a point source. Then, the light from a point source falls into a collimator in a spectrograph. The collimator is usually an off-axis paraboloid, so that it make the light parallel and redirects the light towards into diffraction grating. Diffraction grating dispersed the element of light in different wavelength into different direction. Dispersing light will be recorded on the detector, such as a glass photographic plate or a CCD detector. Beside these optical instrument, a spectrograph need to have a comparison lamp. This lamp is at rest with respect to the spectrograph and it emits know spectral lines. These spectral lines are used as a calibrator for observed spectra.

2.3.2 HERCULES spectrograph

The observational part of this research was conducted by Dr. Siramas Komonjinda at Mt John Observatory (MJUO) using the 1-m McLellan telescope and HERCULES spectrograph during October 2004 to August 2007. The 1-m McLellan telescope is a Dall-Kirkharn reflecting telescope built in 1986. There are two Cassegrain foci available at $f/7.7$ and $f/13.5$.

The HERCULES spectrograph whose name stands for High Efficiency and Resolution Canterbury University Large Echelle Spectrograph (Hearnshaw et al. 2002), is one of the world's first vacuum echelle spectrographs. It sit in an insulated room inside a vacuum tank about 20 meters from the telescope. Light is fed to HERCULES along optical fibers from the fibre-feed module that is attached to the telescope at the $f/13.5$ Cassegrain focus.

On the 4.5-m length optical bench inside HERCULES are housed the collimator,

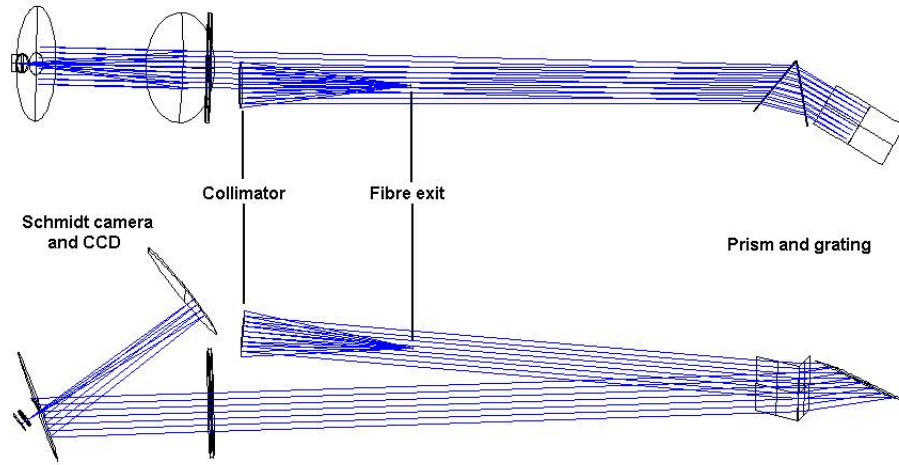


Figure 2.11: Optical design of the HERCULES spectrograph. (Komonjinda, 2008)

prism, echelle grating, Schmidt corrector plate, Schmidt camera, and fold mirror. These optical instruments are installed inside the vacuum tank (2-3 torr) with a temperature control and the spectrograph would have no moving parts. The collimator used for HERCULES is a 210-mm diameter paraboloid with focal length of 783 mm. the cross-dispersion prism is a BK7 prism with an apex angle of $\theta_P = 49.50^\circ$. Its dimensions is height 276 mm, base 258 mm, and length 255 mm with a mass of 23 kg. The echelle grating has 31.6 gr/mm with a blaze angle (θ_B) = 64.33° ($\tan \theta_B = 2.08$) and its ruled area is 204 by 408 mm.

The Littrow angle is made as small as possible so as to give high peak efficiency while still separating the incident and diffracted beams. HERCULES uses $\theta = 3.0^\circ$

The Schmidt camera is set to correct any aberration. It consist of the BK7 Schmidt plate and a fold mirror is located inside the vacuum tank, the field-flattening lens which acts as a tank's window and a CCD detector. During the observation time of this research, the HERCULES detector was a SITE SI 003 1024×1024 thinned CCD chip with 23 micron square pixels. This chip cannot cover all the focal plane area of the dispersed spectrum. The dispersed area was separated into four regions to match the size of the SITE CCD. The CCD region that was mainly used in this research is called region 2, which covers a wavelength region around 4500-7000 Angstrom, in approximately 48 orders. The CCD region 4 was also position used and is able to record the CaII H and K emission line for the purpose of studying the RS CVn variable star.

Inside the fibre –fed module of HERCULES, there are two standard lamp that can direct light into the fibres. These are a Thorium-Argon (Th-Ar) hollow cathode lamp and a white smooth-field lamp. The Th-Ar spectra are used for the purpose of wavelength calibration. The white lamp spectrum is used for the order tracing and flat fielding.



ลิขสิทธิ์มหาวิทยาลัยเชียงใหม่
Copyright© by Chiang Mai University
All rights reserved